U.S. ARMY RDECOM

DESIGN OF A CORROSION DETECTION SYSTEM FOR A SHELTER STRUCTURE

Jean P. Vreuls
Engineering Directorate
Aviation and Missile Research, Development,
and Engineering Center

And

Thomas C. Null
Avnik Defense Solutions, Inc.
7262 Governors West Drive, Suite 102
Huntsville, AL 35806

And

Danny L. Parker
Modern Technology Solutions, Inc.
360 Quality Circle NW
Huntsville, AL 35806

August 2015

AMRDEC

REPORT DOCUMENTATION PAGE

1. AGENCY USE ONLY	2. REPORT DATE August 2015	3. REPORT TYPE AND DATES COVERED Final

4. TITLE AND SUBTITLE

Design of a Corrosion Detection System for a Shelter Structure

5. FUNDING NUMBERS

6. **AUTHOR**(S)

Jean P. Vreuls, Thomas C. Null, and Danny L. Parker

7. PERFORMING ORGANIZATION NAME(S) AND ADDRESS(ES)

Commander, U.S. Army Research, Development, and
   Engineering Command
ATTN: RDMR-SER
Redstone Arsenal, AL 35898-5000

8. PERFORMING ORGANIZATION REPORT NUMBER

SR-RDMR-ED-15-01

9. SPONSORING / MONITORING AGENCY NAME(S) AND ADDRESS(ES)

10. SPONSORING / MONITORING AGENCY REPORT NUMBER

11. SUPPLEMENTARY NOTES

12a. DISTRIBUTION / AVAILABILITY STATEMENT

Approved for public release; distribution is unlimited.

12b. DISTRIBUTION CODE

A

13. ABSTRACT *(Maximum 200 Words)*

The location of sensors on a structure has a large impact on the success of any damage detection method. Heuristically placing many sensors on a structure does not guarantee damage will be detected. By design, optimally placed sensors specific to the structure, the number of sensors needed to detect damage can be limited [1]. This has many benefits including reducing data confusion, as well as minimizing the weight added to the structure.

14. SUBJECT TERMS

Diagnostic Prognostic Lab (DPL), Structural Health Monitoring (SHM), Finite Element Model (FEM)

15. NUMBER OF PAGES

13

16. PRICE CODE

17. SECURITY CLASSIFICATION OF REPORT UNCLASSIFIED	18. SECURITY CLASSIFICATION OF THIS PAGE UNCLASSIFIED	19. SECURITY CLASSIFICATION OF ABSTRACT UNCLASSIFIED	20. LIMITATION OF ABSTRACT SAR

Title: *Design of a Corrosion Detection System for a Shelter Structure*

Authors: Thomas C. Null
Danny L. Parker
Jean Vreuls

ABSTRACT

The location of sensors on a structure has a large impact on the success of any damage detection method. Heuristically placing many sensors on a structure does not guarantee damage will be detected. By design, optimally placed sensors specific to the structure, the number of sensors needed to detect damage can be limited [1]. This has many benefits including reducing data confusion, as well as minimizing the weight added to the structure.

INTRODUCTION

The US Army has stated technology gaps in monitoring items in both short and long term storage; this paper will focus on monitoring of the S-280 shelter. Since the US Army Aviation and Missile Research, Development, and Engineering Center (AMRDEC) Diagnostic Prognostic Lab (DPL) has a track record of applying optimal-sensor-placement-strategy to structures [2], the laboratory was tasked with designing a structural health monitoring (SHM) system to monitor a S-280 shelter. Optimal-sensor-placement-strategy, Optimized SHM has demonstrated 6-7 times the sensitivity with 50 percent fewer sensor than heuristically designed systems with the same design goals.

The optimal-sensor-placement-strategy of the SHM was demonstrated to correlate with corrosion damage and corrosion damage growth; hence, corrosion detection addressing the storage monitoring gap by giving insight into the structural conditions of the shelter while in storage. Shelter maintainers claim that, if they know exactly where the corrosion is present, they would save ~30% during the reset process.

The goal of this report is to show the process of optimally placing actuators and sensors to detect damage due to corrosion. While the original effort was to include field testing, the field testing did not occur due to a change in tasking; instead the effort implemented simulated damage in the Finite Element Model (FEM).

Thomas C. Null, Danny L. Parker, AVNIK Defense, Huntsville, AL, 35806
Jean P. Vreuls, AMRDEC, Redstone Arsenal, Huntsville, AL, 35806, USA

This report covers the SHM corrosion detection task to include: optimal sensor placement theory; corrosion metric test validation, FEM creation for the S-280 shelter, generation of a Pareto front for actuator and sensor placement designs; and the results of using an optimized design for simulated corrosion detection.

The framework for designing an optimal health monitoring system is always the same regardless of the part. Following FEM development, model accuracy is determined via modal analysis on the test article. When the model sufficiently represents the dynamics of the test article, the optimization criterion is analyzed and model inaccuracies are taken into account. The user then defines a damage metric that is physically measurable and design validating simulations are performed. Finally, sensors are attached to the structure in the optimal locations and tested.

OPTIMAL SENSOR PLACEMENT THEORY

Assume that the physical phenomena (elastic, thermal, electromagnetic, etc.) of interest for the structure can be modeled adequately as a linear time invariant (LTI) dynamical system in state-space form; as given in (1) where x(t) is the state vector, u(t) is the actuator signal vector, y(t) is the sensor signal vector, and x(0) is the initial state condition.

$$\dot{x}(t) = Ax(t) + Bu(t)$$
$$y(t) = Cx(t) + Du(t) \tag{1}$$

The matrices A, B, C, and D represent the system dynamics, actuator influence, sensor coupling, and direct feed through effects, respectively. To highlight a particular case, consider the familiar second-order vector form FEM of an elastic structure; given in (2), where *M*, *G*, and *K*, are the mass, damping, and stiffness matrices, respectively.

$$M\ddot{z}(t) + G\dot{z}(t) + Kz(t) = Fu(t) \tag{2}$$

Here, the matrix *F* maps the actuator signals into the usual force vector and should be thought of as specifying where independent forces are applied to the structure. The vector z consists of the translational and rotational degrees-of-freedom (DOFs). Solving (2) as a system of first order equations results in (3) [3].

$$A = \begin{bmatrix} 0 & I \\ -M^{-1}K & -M^{-1}G \end{bmatrix}, B = \begin{bmatrix} 0 \\ M^{-1}F \end{bmatrix} \tag{3}$$

In the case where accelerometers are used for sensing, (4) applies where C_a is a matrix specifying the locations of the accelerometers and *F* is a matrix specifying the locations of the actuators.

$$y(t) = -C_a M^{-1}[K\ G]x(t) + C_a M^{-1}Fu(t) \tag{4}$$

Our goal in this work is to optimally position accelerometers and actuators on a structure to detect changes in the structure's dynamics: i.e., to determine the best matrices C_a and *F*. This corresponds to finding the best DOFs to measure and excite. The excitation is chosen to be a zero-mean, Gaussian band-limited white noise with

a covariance matrix Q_u. The steady-state response of the system defined in (1) to this input is given by (5), where Q_x is the steady-state covariance of the state vector x and can be shown to be the solution to the matrix Lyapunov equation given by (6).

$$Q_y = CQ_xC^T + DQ_uD^T \tag{5}$$

$$AQ_x + Q_XA^T + BQ_uB^T = 0 \tag{6}$$

Readily available numerical algorithms exist to solve (6). To optimally position the sensors and actuator when the damage location is known, maximize the matrix 2-norm of the sensitivity of the steady-state sensor covariance Q_y with respect to parametric variations in the system matrices A, B, C, and D. To optimally position the sensors and actuator when the damage location is unknown or when wanting to remain sensitive to unpredicted damage locations, maximize the singular value decomposition of the steady-state covariance matrix Q_o from (7). An alternative solution is to normalize the Eigen vectors and maximize the minimum singular value of the Hankle Matrix. The Hankle Matrix is formed by simply multiplying Q_x and Q_o.

$$A^TQ_0 + Q_0A + C^TQ_uC = 0 \tag{7}$$

To put this plainly, the algorithm maximizes the change in the output signal when damage develops in the structure. In general, the entries of these matrices are determined by the geometry and physical properties of the materials used in the structure to be monitored. Other sensitivity measures are possible, but this one is sensitive to a large space of changes and is mathematically represented by (8) where $\partial Q_x/\partial p$ is the solution to (9) and p is a parameter characterizing the effect of damage on the structure. Usually p influences the entries of M, K, and G.

$$\frac{\partial Q_y}{\partial p} = \frac{\partial C}{\partial p}Q_xC^T + C\frac{\partial Q_x}{\partial p}C^T + CQ_x\frac{\partial C^T}{\partial p} + \frac{\partial D}{\partial p}Q_uD^T + D\frac{\partial Q_u}{\partial p}D^T + DQ_u\frac{\partial D^T}{\partial p} \tag{8}$$

$$\frac{\partial A}{\partial p}Q_x + A\frac{\partial Q_x}{\partial p} + \frac{\partial Q_x}{\partial p}A^T + Q_x\frac{\partial A^T}{\partial p} + \frac{\partial B}{\partial p}Q_uB^T + BQ_u\frac{\partial B^T}{\partial p} = 0 \tag{9}$$

Using these equations, along with a finite-dimensional model of a structure, a multi-objective optimization algorithm, such as a genetic algorithm, can be used to find the optimal locations of the sensors and actuators.

CORROSION DEMONSTRATIONS

To demonstrate the correlation between the damage metric and actual corrosion (as opposed to mass changes) two test coupons were instrumented and subjected to a salt fog chamber. The coupons were 3" x 5" unprotected sheets of steel; three uni-axis accelerometers and one piezo were bonded on each coupon, and then placed in a salt fog chamber for 69 hours under salt mix conditions of ASTM G85-A5 and spray conditions of ASTM B117. Data were collected and processed every two minutes during the test. A clear correlation between the damage metric and corrosion
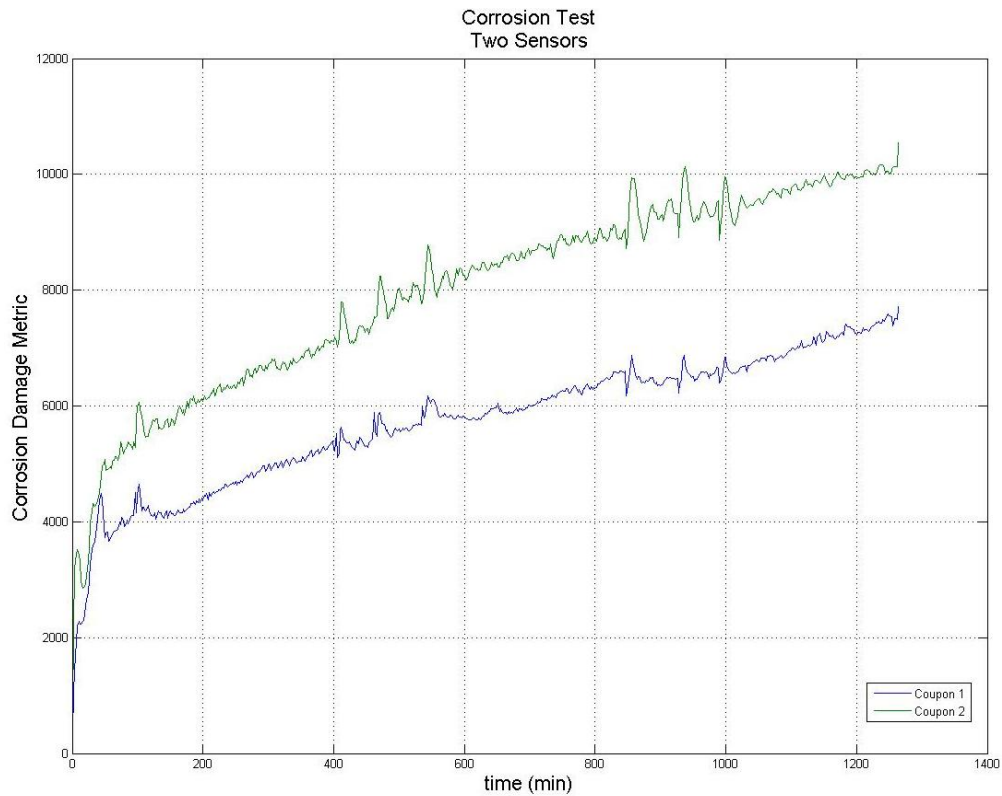
Figure 1. Damage Metric vs. Time for Coupons in Salt Fog Chamber.

can be seen in Figure 1. The spikes shown in the figure are due to the test being stopped and the chamber opened, while pictures were taken at set intervals throughout the process.

FEM S-280 SHELTER

Overview

The S-280 Shelter was modeled in Creo Parametric and simplified for easier processing and meshing once the model was imported into ANSYS. Once imported, the structure was prepared for meshing and meshed with hexahedral volume elements. Lastly, modal analysis was performed and the first 12 modes and mode shapes requested from the analysis captured.

Model Properties and Simulation Details

The model, built in inches, used standard aluminum with a Young's Modulus (E) of 69 GPa, Poisson's Ratio (ν) of .33 and a density (ρ) of 2700 kg/m^3, and a structure foam estimate. The values of the foam were unknown, so the foam material was varied to observe the effects of the foam properties on the analysis. The initial values for the foam were E = 13.8 MPa, ν = .15, and ρ = 950 kg/m^3. The foam was then varied for the remaining runs; TABLE I. tabulates the values used.

Material	Aluminum	Foam 1	Foam 2	Foam 3	Foam 4	Foam 5	Foam 6
Runs used	All	1,2	3	4	5	6	7
Young's Modulus (MPa)	69,000	13.8	22.2	22.2	22.2	14.5	31.1
Poisson's Ratio	.33	.15	.15	.12	.25	.15	.15
Density (kg/m^3)	2700	950	67	67	67	45	90

TABLE I.   MATERIAL PROPERTIES

The foam data was taken from GE Plastics Engineering Structural Foam Design and Processing Guide. The remaining values were taken from a handout by JSP. The model was meshed with the hexahedral SOLID183 elements which for the frames and skids were set to be solid homogeneous volumes of aluminum. The panels were defined as being layered SOLID183 elements with a foam core and aluminum skins. The walls were 2.06 inches thick and the aluminum skin was .09 inches thick on each side.

The first mesh implemented had element edge lengths of .05 meters (about 2 inches) and was composed of 31,718 elements and 48,281 nodes. The second mesh had element lengths of .025 meters (about 1 inch) and was composed of 174,330 elements and 234,594 nodes. The first run use the first mesh and all follow-on funs used the second mesh. One observation noted is the meshes have too many nodes for the desired application, however, to achieve a good baseline data set to check the foam properties was needed, thus a fine mesh was used.

Procedure

The S-280 Shelter was modeled in Creo Parametric and simplified for easier processing and meshing once the model was imported into ANSYS. Only a quarter of the shelter was modeled to take advantage of the symmetry of the model.

This assembly was then imported into ANSYS using the parasolid format. The Boolean "glue" operation was applied to the model, which was required to merge the areas on volumes with contact and promote connectivity within the model. The model geometry was further simplified to reduce irregular areas that had resulted from the glue operation. The areas and lines were then concatenated to allow for mapped meshing and the model was meshed with hexahedral elements. The modal analysis was chosen and set to extract the first 12 natural frequencies and modes shapes. The symmetry, support, and gravity boundary conditions were applied to the model and the analysis carried out. The mesh of the model was then refined slightly and the analysis re-run. Last, the material properties of the foam were varied and the analysis was re-run for each set to observe the effect that they had upon the natural frequencies and mode shapes.

Results

Once the meshing procedure was completed and the boundary conditions applied, the modal analysis gave the requested results. A total of 7 runs were made, with the goal of strategically varying the properties of the foam and the mesh to get an idea of the effect that they had on the model. The results showed that foam density had the largest effect on the frequency. The effect of changes to the Poisson's Ratio was found to be minimal and the effect of Young's modulus was also found to be small.

OPTIMAL SENSOR DESIGN FOR S-280 SHELTER

Process

Because of the large size of the resulting matrices and iterative nature of the design algorithm, we reduce the number of DOFs in the model as much as possible without appreciable loss of accuracy. Therefore, modal truncation to the band of frequencies of interest and modal participation analysis were used to reduce the DOFs, making the problem workable on a standard PC.

The first step was to calculate all Eigen vectors from 0 to 13 kHz and store those values. Next, a frontend filter was created to force the model to only respond within the physical limits of our actuator (500-8kHz). The Mass and Stiffness matrices were then transformed to the modal domain by a user defined set of Eigen vectors (400-10 kHz). The Damping matrix was created in the modal domain as inversely proportional to the Mass matrix.

The objective function builds the state space matrices (A, B, C, and D) using the modal domain Mass, Stiffness, and Damping matrices as well as the inputs and outputs specified. The inputs define the location of the actuators, which are assumed to be triaxial and the outputs are assumed to be triaxial accelerometers. A modal participation mask is applied to reduce the computational complexity of the model. Only modes that can be excited due to the location of the inputs remain. The frontend filters are added to the state space model (one set for each input axis). Finally, the objective functions are calculated as the negative minimum singular value of the Hankle matrix, the number of inputs, and the number of outputs.

A genetic algorithm (GA) based on NSGA-II was employed to minimize the objective function. NSGA-II is a popular non-dominated sorting GA that addresses the three main deficiencies in the original NSGA: High computational complexity, lack of elitism, and automated diversity preservation. Trials of this algorithm when applying it to a simple beam model proved to be approximately 100 times faster than exhaustive search.

Results

The GA was allowed to run for 32 hours and achieved clear Pareto fronts (Figure 2). The Hankle Objective is plotted as –log10(-x) for display purposes. While the GA is not guaranteed to find the optimal solution, an exhaustive search of the full FEM is not possible and the solution of the GA is far superior to random guessing.

The GA was used to search for a design consisting of up to 12 sensors and 4 actuators, resulting in a Pareto Front. In order to test the results, a baseline was created using the design containing 12 sensors and 4 actuators (Figure 3). A location known to likely corrode was then selected (Figure 4).
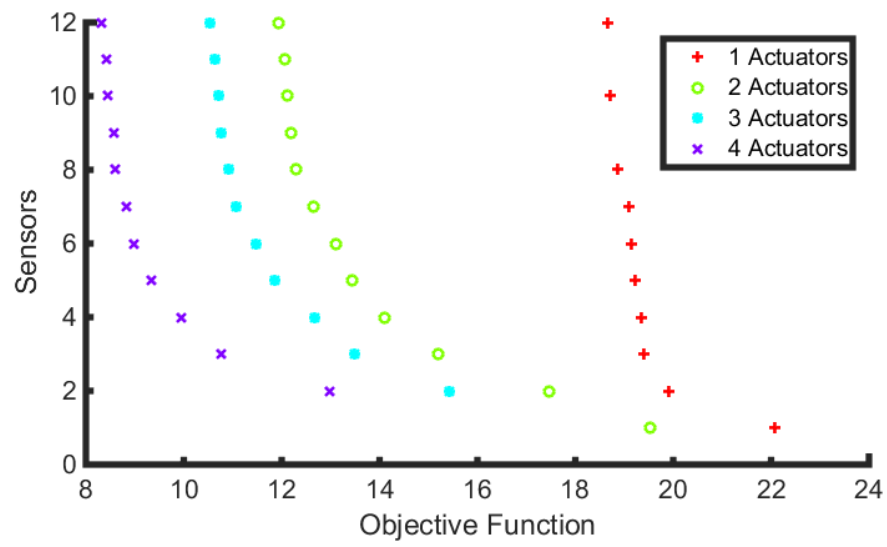
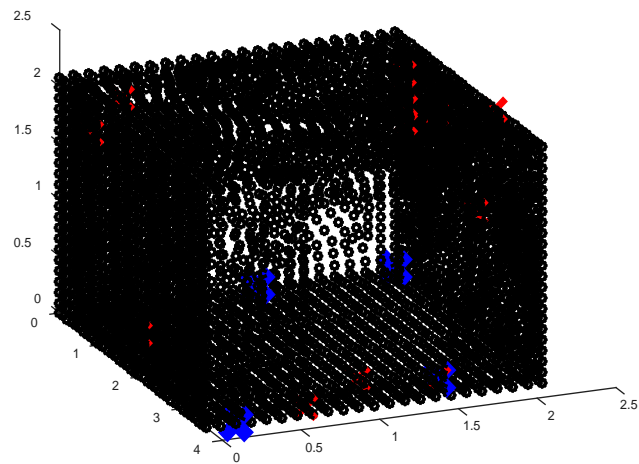Figure 2. Pareto Fronts for S-280 Shelter.

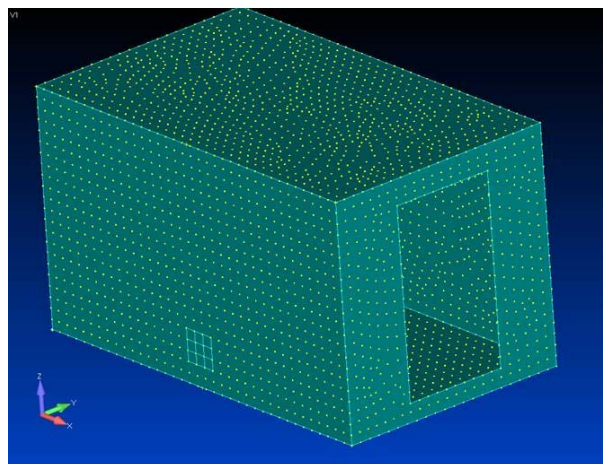Figure 3. 4 actuator 12 sensor design for S-280 Shelter.

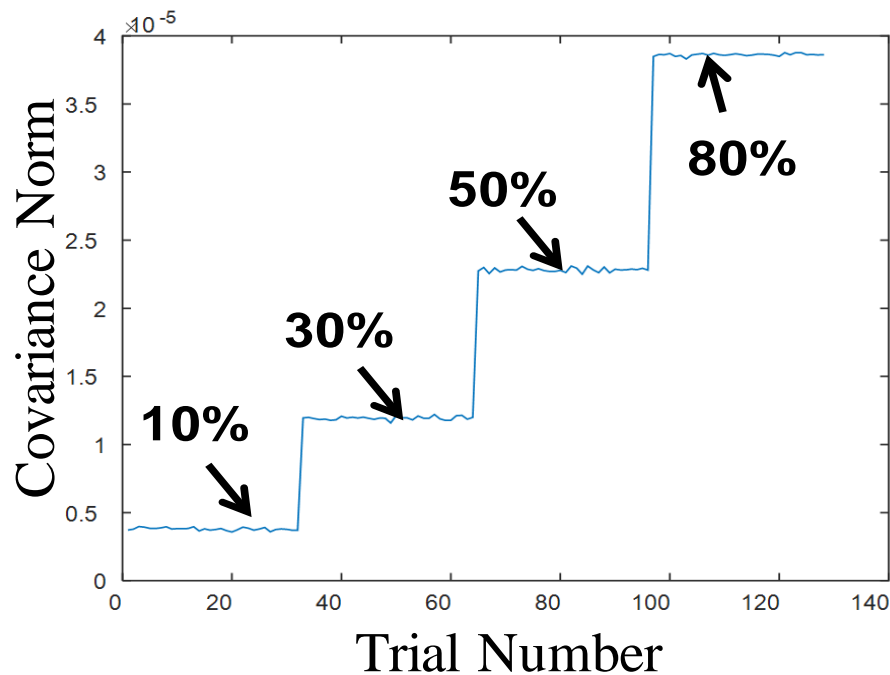
Figure 4. Likely corrosion location.

Figure 5. Detection Metric.

The four nodes associated with the center element were then modified to exhibit 10%, 30%, 50%, and 80% mass loss of this element. This represents a total change in mass of 0.0008%, 0.0024%, 0.0039%, and 0.0063% respectively. A baseline of 100 samples for the undamaged case was then generated and compared against 32 simulations of each of the damaged models; results are seen in Figure 5.

CONCLUSIONS

Optimizing the locations of sensors and actuators has many advantages. The test results herein show that optimally placed sensors should be able to detect corrosion on the S-280 Shelter. By minimizing the number of sensors and actuators added to a structure, this greatly reduces the added weight, reduces the amount of data collected, maximizes sensitivity to damage, and ensures global coverage of detecting damage anywhere on the structure.

REFERENCES

1. W. G. Frazier and D. L. Parker, "Dynamical Systems Research for Vehicle Health Monitoring," in *AeroMat*, Dayton, OH, 2003.
2. D. L. Parker and P. Dussault, "Structural Condition Monitoring of Helicopter Components," in *The 9th International Workshop on Structural Health Monitoring*, Stanford, 2013.
3. C. L. Phillips and R. D. Harbor, Feedback Control Systems, Upper Saddle River: Prentice-Hall, 1996.

INITIAL DISTRIBUTION LIST

		Copies
Defense Systems Information Analysis Center SURVICE Engineering Company 4695 Millennium Drive Belcamp, MD 21017	Ms. Jessica Owens jessica.owens@dsiac.org	Electronic
Defense Technical Information Center 8725 John J. Kingman Rd., Suite 0944 Fort Belvoir, VA 22060-6218	Mr. Jack L. Rike jackie.l.rike.civ@dtic.mil	Electronic
AMSAM-L	Ms. Anne C. Lanteigne hay.k.lanteigne.civ@mail.mil	Electronic
	Mr. Michael K. Gray michael.k.gray7.civ@mail.mil	Electronic
RDMR		Electronic
RDMR-CSI		Electronic
RDMR-SER	Mr. Jean P. Vreuls jean.p.vreuls.civ@mail,mil	Electronic
Avnik Defense Solutions, Inc. 7262 Governors West Drive, Suite 102 Huntsville, AL 35806	Mr. Thomas C. Null thomas.c.null.ctr@mail.mil	Electronic
Modern Technology Solutions, Inc. 360 Quality Circle NW Huntsville, AL 35806	Mr. Danny L. Parker danny.l.parker20.ctr@mail.mil	Electronic